

Dilepton Signal of a Type-II Seesaw at CERN LHC: Reveals a TeV Scale $B - L$ Symmetry

Swarup Kumar Majee*

*Center for Particle Physics and Phenomenology (CP3), Université Catholique de Louvain,
Chemin du Cyclotron 2, B-1348 Louvain-la-Neuve, Belgium*

Narendra Sahu†

Service de Physique Théorique, Université Libre de Bruxelles, 1050 Brussels, Belgium

Abstract

We explore the discovery potential of doubly charged Higgs bosons ($\xi^{\pm\pm}$) at the CERN Large Hadron Collider (LHC). For moderate values of the coupling constants in the original Type-II seesaw model, these doubly-charged Higgs bosons are not accessible at any present or near future collider experiments. In a gauged $B - L$ symmetric model we introduce two triplet scalars to execute a variant of type-II seesaw at the TeV scale. This leads to a clear like-sign dilepton signal in the decay mode of $\xi^{\pm\pm}$ for a small vacuum expectation value ($\lesssim 10^5$ eV) of the triplet scalar $\xi = (\xi^{++}, \xi^+, \xi^0)$ of mass $\lesssim 1$ TeV. To be specific, for a mass range of 200-1000 GeV of $\xi^{\pm\pm}$, the like-sign dilepton signal can be detected at CERN LHC at a center of mass energy 14 TeV with an integrated luminosity, say, $\gtrsim 30 \text{ fb}^{-1}$. The same analysis is also pursued with center of mass energies 7 TeV and 10 TeV as well. We also comment on the decay mode of singly charged scalars and neutral $B - L$ gauge boson in this model.

PACS numbers: 14.60.Pq

*Electronic address: swarup.majee@uclouvain.be

†Electronic address: Narendra.Sahu@ulb.ac.be

I. INTRODUCTION

The CERN Large Hadron Collider (LHC) has already started to set up a new milestone in the high energy physics experiment. Besides Higgs bosons search, different types of TeV scale new physics will also be examined. In this work, we explore one such TeV scale physics necessary to explain the sub-eV neutrino masses, required by the low energy neutrino oscillation data, at the LHC.

The nature of neutrino: Dirac or Majorana, is yet a mystery. If the neutrinos are assumed to be Majorana, then the sub-eV neutrino masses can be generated through the dimension five operator [1]

$$\mathcal{O}_\nu = \frac{HHLL}{\Lambda}, \quad (1)$$

where Λ is the scale of doubly lepton number violation, which can be at any point in between the electroweak scale and GUT scale, H and $L \equiv (\nu_l \ l)_L^T$ are Higgs and lepton doublets of standard model (SM). The gauge structure of the SM implies that the effective dimension five operator (1) can be realized in many extensions of the SM [2]. A popular way of generating it is to invoke the seesaw mechanisms.

If the seesaw is implemented by introducing a singlet heavy fermion (N) per family with hypercharge $Y = 0$, then it is called type-I seesaw [3]. The effective light neutrino mass is then given by

$$M_\nu \equiv M_\nu^I = -m_D M_N^{-1} m_D^T, \quad (2)$$

where m_D is the Dirac mass matrix of the neutrinos connecting to the left-handed neutrinos (ν_L) with the singlet heavy fermion (N) and M_N is the mass matrix in the flavor space of the singlet fermions, which also sets the scale of lepton number violation (Λ). Assuming that $m_D \propto M_u$, the up quark mass matrix, as in the case of $SO(10)$ grand unified theories, the neutrino mass can be given as $M_\nu \simeq m_t^2/M_N$, where m_t is the top quark mass. Conservatively if we take $M_\nu \leq 1$ eV, M_N will then become heavier than 10^{13} GeV which is beyond the reach of any near future colliders. However, one can lower the mass scale of M_N by tuning the Yukawa coupling $Y = m_D/v$, v being the vacuum expectation value (vev) of the SM Higgs H . This loses the philosophy of seesaw ¹, unless the experimental constraints on Y

¹ One can bring down the scale of seesaw by using either dimension-7 [4] or dimension-9 operator [5] for neutrino masses. However, these operators can not be realized within the particle content of minimal

demand so.

If the singlet N in type-I seesaw is replaced by an $SU(2)_L$ triplet heavy fermion Σ with hypercharge $Y = 0$ then it corresponds to type-III seesaw [8] and the effective light neutrino mass is then given by Eq. (2) except M_N is replaced by M_Σ , the mass of Σ . This implies that one can not bring down M_Σ to TeV scale without tuning the Yukawa couplings which connect the left-handed neutrinos to the heavy triplet fermions. However, the advantage of type-III seesaw over type-I seesaw is that the triplet fermions can have gauge interactions and can be copiously produced at collider even though the Yukawa couplings are small. Therefore, the triplet fermions can give rise to distinctive signatures at collider [9], but plagued with a large SM background.

Another way of implementing the seesaw mechanism is to introduce an $SU(2)_L$ triplet scalar Δ with hypercharge $Y = 2$. Then it is called type-II seesaw [10, 11]. The effective light neutrino mass is then given by

$$M_\nu \equiv M_\nu^{II} = f\mu \frac{v^2}{M_\Delta^2}, \quad (3)$$

where M_Δ is the mass of the triplet Higgs scalar Δ , μ is the coupling constant with mass dimension 1 for the trilinear term with the triplet Higgs and two standard model Higgses and f is the Yukawa coupling relating the triplet Higgs with the SM lepton doublets. Both M_Δ and μ are assumed to be of the same order of magnitude and they set the scale (Λ) of lepton number violation and v is the vev of the SM Higgs doublet. Optimistically if we assume $M_\nu \lesssim 1$ eV, then we get $f \lesssim 10^{-3}$ for $M_\Delta \simeq 10^{10}$ GeV. Therefore, the traditional type-II seesaw is far reach from near future colliders. To bring down further the scale of lepton number violation one needs to fine tune the coupling f and/or μ . For example, assuming $\mu \sim M_\Delta$, the Δ mass can be brought to TeV scales only at the cost of $f \sim 10^{-10}$ as it is clear from Eq. (3). Alternatively, taking $f \sim \mathcal{O}(1)$ the sub-eV neutrino masses can be achieved by assuming $M_\Delta \sim v$ and $\mu \sim \mathcal{O}(1)$ eV [12].

Thus from Eq. (3) we see that to bring down the mass scale of Δ to TeV scales one can have two choices. In one case, the Yukawa coupling f can be small, while in the other case the trilinear coupling μ can be small. In the former case, the theory losses its predictivity

type-I seesaw model [3]. By adding extra degrees of freedom to the minimal type-I seesaw model, one can of course implement double [6] and triple type seesaw [7] to realize the scale of seesaw at TeV scale. However, these models are not predictive due to the addition of extra singlets.

as Δ dominantly decays to SM Higgses and rarely to leptons, while in the latter case, it is attractive [12, 13] as the triplet rarely decays to SM Higgses and dominantly decays to SM leptons, which can be verified at near future colliders. In this article we follow the latter approach and propose a variant of type-II seesaw to explain the sub-eV neutrino masses. The proposed seesaw can be accessible at LHC and/or ILC, while keeping the philosophy of seesaw ² intact. This is accomplished by extending the SM with two $SU(2)_L$ triplet scalars Δ and ξ , instead of one super heavy triplet scalar Δ as in the usual type-II seesaw. However, as we will see the number of degrees of freedom in the effective theory are same as that of the original type-II seesaw [11], while the low energy predictions are almost similar to the triplet scalar model [12]. The doubly lepton number violation, required for neutrino Majorana masses, is achieved in a TeV scale gauged $B - L$ symmetric model. As a result, the neutral gauge boson corresponding to $U(1)_{B-L}$ gauge symmetry gives rise to distinctive signatures at collider. In particular, if the $B - L$ gauge boson mass is a few TeV then its on-shell decay can populate doubly and singly charged scalars at collider. Alternatively, if $B - L$ gauge boson mass is less than a TeV then it contributes to the pair production of charged scalars via Drell-Yan process. We then present the relevant collider signature of singly and doubly charged scalars, which can be accessible at CERN LHC.

The paper is organized as follows. In section-II, model independently we present a TeV scale type-II seesaw to explain the sub-eV neutrino masses. In section-III, a gauged $U(1)_{B-L}$ symmetric model is proposed to realize the TeV scale type-II seesaw. We delineate the parameter space of M_ν , allowed by three flavor neutrino oscillation data, in section-IV by imposing the lepton flavor violating constraints. Section-V is devoted to probe the model at LHC through the observation of like-sign dilepton decay of doubly charged scalars. We briefly comment on the decay modes of a singly charged scalars in section-VI. Finally, we conclude in section-VII.

² In many extensions of SM including $SU(2)_L$ singlets and doublets seesaw is realized at TeV scales [14].

II. A TYPE-II SEESAW AT THE TEV SCALE AND SUB-EV NEUTRINO MASSES

To realize the type-II seesaw at the TeV scale let us extend the SM Lagrangian by including two $SU(2)_L$ triplet scalars $\xi(1, 3, 2)$ and $\Delta(1, 3, 2)$, where the quantum numbers in the parentheses are under the SM gauge group $\mathcal{G}_{SM} \equiv SU(3)_C \times SU(2)_L \times U(1)_Y$. While the mass scale of ξ is at the TeV scale, the mass of Δ is assumed to be at the GUT scale. We assume that the $B - L$ quantum number of ξ and Δ to be 2 and 0 respectively. As a result, the $B - L$ conserving terms in the Lagrangian involving ξ and Δ can be given as [13]

$$- \mathcal{L}_{B-L} \supset M_{\Delta}^2 \Delta^{\dagger} \Delta + M_{\xi}^2 \xi^{\dagger} \xi + \frac{1}{\sqrt{2}} \left[\mu \Delta^{\dagger} H H + f_{\alpha\beta} \xi L_{\alpha} L_{\beta} + \text{h.c.} \right], \quad (4)$$

where H and L are the SM Higgs and lepton doublets respectively. After the Electroweak (EW) phase transition Δ acquires a small induced vev ³

$$\langle \Delta \rangle = -\mu \frac{v^2}{\sqrt{2} M_{\Delta}^2}, \quad (5)$$

where $v = \langle H \rangle$. Thus for $\mu \sim M_{\Delta} \sim 10^{12}$ GeV and $v = 246$ GeV one can have a small vev for Δ . However, the vev of Δ does not break lepton number since the $B - L$ quantum number of Δ is zero. Therefore, we can not generate Majorana masses for neutrinos until it is broken. To generate Majorana masses we need to break the global $U(1)_{B-L}$ symmetry of the SM without destroying the renormalizability of the theory while ensuring that there is no massless Goldstone boson that can cause conflict with phenomenology. This can be *minimally* achieved by adding a soft term to the Lagrangian (4)

$$- \mathcal{L}_{\Delta\xi} = M_{B-L}^2 \Delta^{\dagger} \xi + \text{h.c.}, \quad (6)$$

where M_{B-L} is assumed to be at the TeV scale in order to explain the sub-eV neutrino masses. The mixing between ξ and Δ can be parameterized by

$$\tan 2\theta = \frac{2M_{B-L}^2}{M_{\Delta}^2 - M_{\xi}^2}. \quad (7)$$

Since $M_{B-L} \sim M_{\xi}$ and $M_{\Delta} \gg M_{\xi}, M_{B-L}$, the mixing angle is simply

$$\theta \simeq \frac{M_{B-L}^2}{M_{\Delta}^2} \sim 10^{-18}, \quad (8)$$

³ However, ξ can not acquire any vev since its coupling with SM Higgs is forbidden by conservation of lepton number.

where we have used $M_{B-L} = 10^3$ GeV and $M_\Delta = 10^{12}$ GeV. As a result the mass eigen states are:

$$\xi' = \xi - \left(\frac{M_{B-L}^2}{M_\Delta^2} \right) \Delta \sim \xi \quad \text{and} \quad \Delta' = \Delta + \left(\frac{M_{B-L}^2}{M_\Delta^2} \right) \xi \sim \Delta. \quad (9)$$

Since the soft term (6) introduces an explicit lepton number violation through the mixing between Δ and ξ , the left-handed neutrinos can acquire masses. The effective L -number violating Lagrangian involving ξ and Δ is then given by

$$- \mathcal{L}_{B-L} = M_\Delta^2 \Delta^\dagger \Delta + M_\xi^2 \xi^\dagger \xi + \frac{1}{\sqrt{2}} \left(f_{\alpha\beta} \xi L_\alpha L_\beta + \mu \frac{M_{B-L}^2}{M_\Delta^2} \xi^\dagger H H - f_{\alpha\beta} \frac{M_{B-L}^2}{M_\Delta^2} \Delta L_\alpha L_\beta + \mu \Delta^\dagger H H + \text{h.c.} \right) \quad (10)$$

We, thus, see that ξ couples to HH with a small mass dimension coupling: $\mu M_{B-L}^2 / M_\Delta^2 \sim \mathcal{O}(1)$ eV, while its coupling to lepton doublets can in principle be $\mathcal{O}(1)$. Similarly, Δ couples to LL with a small dimensionless coupling: $M_{B-L}^2 / M_\Delta^2 \sim 10^{-18}$, while its coupling to HH is as large as its mass scale. After EW phase transition the triplet scalar ξ acquires a vev:

$$\langle \xi \rangle = -\mu \left(\frac{v^2}{\sqrt{2} M_\Delta^2} \right) \left(\frac{M_{B-L}^2}{M_\xi^2} \right). \quad (11)$$

Since $M_{B-L} \sim M_\xi$, from Eqs. (5) and (11) it is evident that $\langle \xi \rangle \sim \langle \Delta \rangle$, although they have orders of magnitude difference in their masses.

Let us explicitly write the bi-lepton coupling ξLL as:

$$- \mathcal{L}_\nu = \frac{1}{\sqrt{2}} f_{\alpha\beta} \overline{L}_\alpha^c i\tau_2 \xi L_\beta + \text{h.c.} = \frac{1}{2} f_{\alpha\beta} \left[\sqrt{2} \overline{\ell}_\alpha^c P_L \ell_\beta \xi^{++} + (\overline{\ell}_\alpha^c P_L \nu_\beta + \overline{\ell}_\beta^c P_L \nu_\alpha) \xi^+ + \sqrt{2} \overline{\nu}_\alpha^c P_L \nu_\beta \xi^0 + \text{h.c.} \right], \quad (12)$$

where we have used the matrix form of triplet scalar:

$$\xi = \begin{pmatrix} \frac{\xi^+}{\sqrt{2}} & \xi^{++} \\ \xi^0 & -\frac{\xi^+}{\sqrt{2}} \end{pmatrix}. \quad (13)$$

From Eq. (12), we get the Majorana mass matrix of the neutrinos:

$$(M_\nu)_{\alpha\beta} = \sqrt{2} f_{\alpha\beta} \langle \xi \rangle = f_{\alpha\beta} \left(\frac{-\mu v^2}{M_\Delta^2} \right) \left(\frac{M_{B-L}^2}{M_\xi^2} \right). \quad (14)$$

Thus for $M_{B-L} \sim M_\xi$, $\mu \sim M_\Delta \sim 10^{12}$ GeV and $v = 246$ GeV, we can generate $\mathcal{O}(1)$ eV neutrino masses as required by the laboratory, solar and atmospheric neutrino experiments. Note that the suppression for neutrino mass in Eq. (14) comes from the ‘‘small mixing

$\theta = M_{B-L}^2/M_\Delta^2$ between Δ and ξ . This is in contrast to the original type-II seesaw, where the suppression for neutrino mass is provided by the mass scale of lepton number violating triplet itself. This is the basic difference between our proposed model and the original type-II seesaw [10, 11]. Since the mass of ξ in our model is at the TeV scale, its like-sign dilepton signature can be studied at CERN LHC, which is almost background free.

III. GAUGED $U(1)_{B-L}$ SYMMETRY AND TEV SCALE TYPE-II SEESAW

In order to elaborate our claim in the previous section let us consider a gauged $U(1)_{B-L}$ symmetric model. The $B - L$ gauge symmetry is allowed to break by $\phi_{B-L}(1, 1, 0, -1)$ at a TeV scale, where the quantum numbers in the parenthesis are under the gauge group $\mathcal{G}_{SM} \times U(1)_{B-L}$. As in the section-II, the $B - L$ quantum numbers of Δ and ξ are taken to be 0 and 2 respectively. Then the relevant $B - L$ conserving Lagrangian can be given as ⁴:

$$-\mathcal{L}_{B-L} \supset \frac{1}{\sqrt{2}} \left[\mu \Delta^\dagger H H + f_{\alpha\beta} \xi L_\alpha L_\beta \right] + y \phi_{B-L}^2 \Delta^\dagger \xi + \text{h.c.} \quad (15)$$

As in section-II, we assume M_ξ is at the TeV scale and $M_\Delta \gg M_\xi$. Before ϕ_{B-L} acquires a vev, there is no mixing between ξ and Δ . At TeV scale ϕ_{B-L} acquires a VEV and provides a mixing between Δ and ξ , which is given by the parameter $M_{B-L}^2 = y \langle \phi_{B-L} \rangle^2$. As a result lepton number violates by two units and generates a Majorana neutrino mass: $(M_\nu)_{\alpha\beta} = \sqrt{2} f_{\alpha\beta} \langle \xi \rangle$. The vev of ξ can be obtained by minimizing the scalar potential:

$$\begin{aligned} V(\Delta, \xi, \phi_{B-L}, H) = & M_\Delta^2 \Delta^\dagger \Delta + \lambda_\Delta (\Delta^\dagger \Delta)^2 + M_\xi^2 (\xi^\dagger \xi) + \lambda_\xi (\xi^\dagger \xi)^2 + \lambda_{\Delta\xi} (\Delta^\dagger \Delta) (\xi^\dagger \xi) \\ & + M_\phi^2 (\phi_{B-L}^\dagger \phi_{B-L}) + \lambda_\phi (\phi_{B-L}^\dagger \phi_{B-L})^2 + M_H^2 H^\dagger H + \lambda_H (H^\dagger H)^2 \\ & + \lambda_{\phi H} (H^\dagger H) (\phi_{B-L}^\dagger \phi_{B-L}) + \lambda_{\Delta\phi} (\Delta^\dagger \Delta) (\phi_{B-L}^\dagger \phi_{B-L}) + \lambda_{\xi\phi} (\xi^\dagger \xi) (\phi_{B-L}^\dagger \phi_{B-L}) \\ & + \lambda_{\Delta H} (\Delta^\dagger \Delta) (H^\dagger H) + \lambda_{\xi H} (\xi^\dagger \xi) (H^\dagger H) + \mu \Delta^\dagger H H + y \phi_{B-L}^2 \Delta^\dagger \xi + \text{h.c.} \end{aligned} \quad (16)$$

where $\lambda_\Delta, \lambda_\xi, \lambda_\phi, \lambda_H > 0$ and $\lambda_{\Delta\xi} > -2\sqrt{\lambda_\Delta \lambda_\xi}$, $\lambda_{\Delta\phi} > -2\sqrt{\lambda_\Delta \lambda_\phi}$, $\lambda_{\xi\phi} > -2\sqrt{\lambda_\xi \lambda_\phi}$, $\lambda_{\phi H} > -2\sqrt{\lambda_\phi \lambda_H}$, $\lambda_{\Delta H} > -2\sqrt{\lambda_\Delta \lambda_H}$ and $\lambda_{\xi H} > -2\sqrt{\lambda_\xi \lambda_H}$ are required for vacuum stability. Assuming $\langle \Delta \rangle \equiv u_\Delta \ll \langle H \rangle$ and $\langle \xi \rangle \equiv u_\xi \ll \langle H \rangle$, from Eq. (16) we get

$$u_\Delta = -\mu \frac{v^2}{M_\Delta^2} \quad \text{and} \quad u_\xi = -\frac{y v_{B-L}^2}{M_\xi^2 + \lambda_{\phi\xi} v_{B-L}^2 + \lambda_{\xi H} v^2} u_\Delta, \quad (17)$$

⁴ The mixing between Δ and ξ , while keeping lepton number conserved, can also be achieved by introducing the renormalisable term $\mu' \phi_{B-L} \Delta^\dagger \xi$, where the $B - L$ quantum number of ϕ_{B-L} is -2. In that case by assuming $\mu' \langle \phi_{B-L} \rangle \sim M_\xi^2$, one can achieve $\langle \xi \rangle \sim \langle \Delta \rangle$.

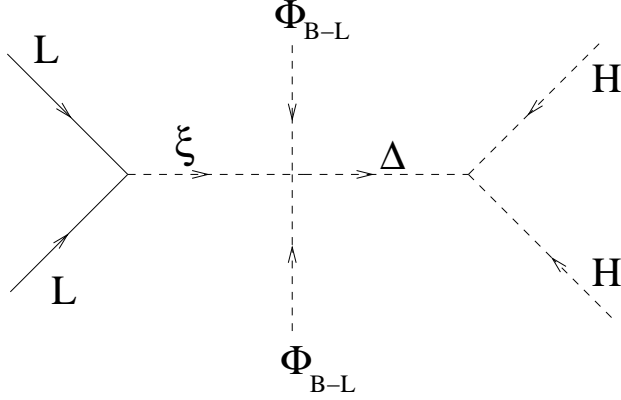


FIG. 1: Neutrino Majorana mass generated through the Modified type-II seesaw in a $U(1)_{B-L}$ symmetric model.

where $v_{B-L} = \langle \phi_{B-L} \rangle$ and $v = \langle H \rangle$. Thus from Eq. (17) we see that for $M_{B-L}^2 = yv_{B-L}^2 \sim M_\xi^2$ we get $u_\Delta \sim u_\xi$. As in the case of type-II seesaw, if we assume that $\mu \sim M_\Delta \sim 10^{10}$ GeV and $v = \langle H \rangle = \mathcal{O}(100)$ GeV then one can generate sub-eV neutrino masses for low energy neutrinos, provided that the ratio: $(M_\xi/M_{B-L}) \sim \mathcal{O}(1)$. This is an important point to be noticed in contrast to the usual type-II seesaw where one allows the explicit lepton number violating couplings ($\mu\Delta^\dagger HH + f\Delta LL$) of a super heavy triplet scalar Δ making almost impossible to test type-II seesaw at collider. Instead here we are making use of two triplet scalars: Δ and ξ so that one is a super heavy scalar (Δ) and other scalar (ξ) is at the TeV scale. Their mixing gives rise to neutrino masses as shown in Fig. (1). From there we see that ξ strongly couples to SM lepton doublets, while its coupling to SM Higgs doublets is suppressed by Δ mass.

Minimizing the scalar potential (16) we get the true minimum for $\langle H \rangle = v$ and $\langle \phi_{B-L} \rangle = v_{B-L}$ as:

$$v = \sqrt{\frac{\lambda_{\phi H} M_\phi^2 - 2\lambda_\phi M_H^2}{4\lambda_\phi \lambda_H - \lambda_{\phi H}^2}}, \quad \text{and} \quad v_{B-L} = \sqrt{\frac{\lambda_{\phi H} M_H^2 - 2\lambda_H M_\phi^2}{4\lambda_\phi \lambda_H - \lambda_{\phi H}^2}}. \quad (18)$$

The electroweak vacuum is then given by a linear combination of v and v_{B-L} :

$$v_{EW} = v \cos \Theta - v_{B-L} \sin \Theta = 246 \text{ GeV} \quad \text{and} \quad v' = v \sin \Theta + v_{B-L} \cos \Theta. \quad (19)$$

Thus for non-zero mixing between v and v_{B-L} we can achieve the EW symmetry (i.e. $v_{EW} = 0$) in the limit $\tan \Theta = v/v_{B-L}$.

Since mass of Δ is $\mathcal{O}(10^{12})$ GeV, as required by the sub-eV masses of neutrinos, it gets

decoupled from the rest of the scalar fields. On the other hand, the mixing between ξ and ϕ_{B-L} , and ξ and H are of $\mathcal{O}(u_\xi/v) \sim 10^{-11}$ as the vev of ξ is $\mathcal{O}(1)$ eV, required by the sub-eV neutrino masses. Therefore, the only significant mixing occurs between H and ϕ_{B-L} .

Since Δ is heavy and decoupled from the rest of the scalars, the number of real scalar degrees of freedom that appear in the low energy effective theory are 12 (four from the SM Higgs H , two from the $B-L$ Higgs ϕ_{B-L} and six from the triplet scalar ξ). Out of which four degrees of freedom are eaten by the gauge bosons W^\pm , Z and Z_{B-L} and hence making themselves heavy. As a result in the low energy effective theory we have 8 physical scalars, namely $\xi^{\pm\pm}$, ξ^\pm , $\text{Re}\xi^0$, $\text{Im}\xi^0$, h_{B-L} and h , where h is the SM like Higgs and h_{B-L} is the $B-L$ like Higgs.

A. Masses and Mixing of ϕ_{B-L} and H

The quantum fluctuations around the minimum can be given as

$$\phi_{B-L} = v_{B-L} + h'_{B-L} \quad \text{and} \quad H = \begin{pmatrix} 0 \\ v + h' \end{pmatrix}. \quad (20)$$

Now using (20) in Eq. (16) we get the mass matrix for h' and h'_{B-L} as:

$$\mathcal{M}^2(h', h'_{B-L}) = \begin{pmatrix} 2\lambda_H v^2 & \lambda_{\phi H} v_{B-L} v \\ \lambda_{\phi H} v_{B-L} v & 2\lambda_\phi v_{B-L}^2 \end{pmatrix}, \quad (21)$$

where the coupling $\lambda_{\phi H}$ decides the mixing between h' and h'_{B-L} Higgses, which can be parameterized by:

$$\tan 2\gamma = \frac{\lambda_{\phi H} v_{B-L} v}{\lambda_\phi v_{B-L}^2 - \lambda_H v^2}. \quad (22)$$

The above equation shows that the mixing angle γ between h'_{B-L} and h' vanishes if either $\lambda_{\phi H} \rightarrow 0$ or $v_{B-L} \gg v$. While for a finite mixing, the masses of the physical Higgses can be obtained by diagonalising the mass matrix (21) and is given by:

$$\begin{aligned} M_h^2 &= (\lambda_H v^2 + \lambda_\phi v_{B-L}^2) - \frac{1}{2} \sqrt{4(\lambda_H v^2 - \lambda_\phi v_{B-L}^2)^2 + 4(\lambda_{\phi H} v_{B-L} v)^2} \\ M_{h_{B-L}}^2 &= (\lambda_H v^2 + \lambda_\phi v_{B-L}^2) + \frac{1}{2} \sqrt{4(\lambda_H v^2 - \lambda_\phi v_{B-L}^2)^2 + 4(\lambda_{\phi H} v_{B-L} v)^2}. \end{aligned} \quad (23)$$

corresponding to the mass eigen states h and h_{B-L} . Due to the mixing between h and h_{B-L} , their couplings to SM fermions and gauge bosons can be given as:

$$Y_{hff} = i \left(\frac{m_f}{v} \right) \cos \gamma, \quad Y_{h_{B-L}ff} = i \left(\frac{m_f}{v} \right) \sin \gamma$$

$$\begin{aligned}
g_{hWW} &= -i \left(\frac{2M_W^2}{v} \right) \cos \gamma, & g_{h_{B-L}WW} &= -i \left(\frac{2M_W^2}{v} \right) \sin \gamma \\
g_{hZZ} &= -i \left(\frac{2M_Z^2}{v} \right) \cos \gamma, & g_{h_{B-L}ZZ} &= -i \left(\frac{2M_Z^2}{v} \right) \sin \gamma \\
g_{hZ_{B-L}Z_{B-L}} &= -i \left(\frac{2M_{Z_{B-L}}^2}{v_{B-L}} \right) \sin \gamma, & g_{h_{B-L}Z_{B-L}Z_{B-L}} &= -i \left(\frac{2M_{Z_{B-L}}^2}{v_{B-L}} \right) \cos \gamma
\end{aligned} \tag{24}$$

where m_f is the mass of the SM fermion f and M_W , M_Z , $M_{Z_{B-L}}$ are masses of W, Z and $U(1)_{B-L}$ gauge boson respectively.

B. Mass and Decay width of Z_{B-L} Gauge Boson

The neutral $B-L$ gauge boson, Z_{B-L} , gets a mass from the vev of the $B-L$ Higgs ϕ_{B-L} . This can be derived explicitly from the kinetic term, $(D_\mu \phi_{B-L})^\dagger (D_\mu \phi_{B-L})$, where

$$D_\mu = \partial_\mu - i\frac{g}{2}\tau_a W_\mu^a - i\frac{g'}{2}Y B_\mu - ig_{B-L}Y_{B-L}(Z_{B-L})_\mu. \tag{25}$$

The Y_{B-L} in the above equation is the $B-L$ charge associated with ϕ_{B-L} and $(Z_{B-L})_\mu$ is the new $U(1)_{B-L}$ gauge boson. Note that there is no tree level mixing between the SM Z boson and Z_{B-L} . Therefore, they can leave distinctive signatures at collider ⁵.

Now expanding the kinetic term using Eq. (25), one gets the mass of Z_{B-L} to be $M_{Z_{B-L}} = g_{B-L}v_{B-L}$. The non observation of Z_{B-L} gauge boson at CDF [17] gives a lower bound on its mass to be $M_{Z_{B-L}} \gtrsim 800$ GeV, while from LEP-II [15] we have

$$\frac{M_{Z_{B-L}}}{g_{B-L}} > 6 \text{ TeV}. \tag{26}$$

Thus the above two bounds agrees with each other for $g_{B-L} > 0.1$. The agreement also implies that $v_{B-L} > \mathcal{O}(\text{TeV})$.

From Eq. (25), we see that Z_{B-L} couples to all the SM leptons and quarks as they carry non-zero $B-L$ quantum numbers and the strength of the coupling is proportional to the corresponding $B-L$ quantum number. As a matter of fact, Z_{B-L} dominantly decays to a pair of leptons since the $B-L$ quantum number of a lepton is -1, while its decay to a pair of quarks is sub-dominant since the $B-L$ quantum number of a quark is 1/3. Assuming that

⁵ Collider signature of $U(1)'$ gauge boson has been studied extensively in the literature [15, 16].

$M_{Z_{B-L}} < M_\xi, M_{h_{B-L}}$, the branching ratio of the decay of Z_{B-L} to a pair of charged leptons can be given as

$$\text{BR}(Z_{B-L} \rightarrow \ell^+ \ell^-) = \frac{\Gamma_{Z_{B-L} \rightarrow \ell^+ \ell^-}}{\sum_f \Gamma_{Z_{B-L} \rightarrow \bar{f} f}} \simeq 15.2\%, \quad (27)$$

where ℓ stands for each individual generation of charged lepton and f stands for the SM fermions. Thus we see that the branching ratio of $Z_{B-L} \rightarrow \ell^+ \ell^-$ is significantly larger than the corresponding SM branching fraction $BR(Z \rightarrow \ell^+ \ell^-) \simeq 3.4\%$. Hence for $M_{Z_{B-L}} \sim \mathcal{O}(1)$ TeV, the signature of Z_{B-L} can be studied at LHC through the decay $Z_{B-L} \rightarrow \ell^+ \ell^-$. Alternatively, if $M_{Z_{B-L}} > M_\xi, M_{h_{B-L}}$, then the total decay width of Z_{B-L} increases as it additionally decays to $h_{B-L} h_{B-L}$, $\xi^{\pm\pm} \xi^{\mp\mp}$, $\xi^\pm \xi^\mp$ and $\xi^0 \xi^{0*}$. As a result, the branching fraction of the decay of $Z_{B-L} \rightarrow \ell^+ \ell^-$ decreases down to 7.11%. However, it strongly decays to doubly charged scalars as the branching fraction of the decay of $Z_{B-L} \rightarrow \xi^{++} \xi^{--}$ is

$$\text{BR}(Z_{B-L} \rightarrow \xi^{++} \xi^{--}) = \frac{\Gamma_{Z_{B-L} \rightarrow \xi^{++} \xi^{--}}}{\sum_f \Gamma_{Z_{B-L} \rightarrow \bar{f} f} + \sum_{h_{B-L}, \xi} \Gamma_{Z_{B-L} \rightarrow (h_{B-L} - \text{pairs}), (\xi - \text{pairs})}} \simeq 21.34\% \quad (28)$$

This implies that for heavy Z_{B-L} the production of $\xi^{++} \xi^{--}$ pair can be enhanced by its on-shell decay, although the production cross-section via Z_{B-L} mediated Drell-Yan process: $\bar{q} q \rightarrow \xi^{++} \xi^{--}$ decreases. We postpone the further discussions on the production of $\xi^{++} \xi^{--}$ pairs in presence of Z_{B-L} gauge boson to section-V.

IV. NEUTRINO OSCILLATION PARAMETERS AND CONSTRAINTS ON $(M_\nu)_{\alpha\beta}$

From Eq. (15), we see that in the effective theory the neutrino mass matrix is given by:

$$M_\nu = \sqrt{2} f u_\xi = U_{\text{PMNS}} M_\nu^{\text{diag}} U_{\text{PMNS}}^T \quad (29)$$

where the mixing matrix U_{PMNS} is the unitary Pontecorvo-Maki-Nakagawa-Sakata matrix and is given by:

$$U_{\text{PMNS}} = \begin{pmatrix} c_{12} c_{13} & s_{12} c_{13} & s_{13} e^{-i\delta_{13}} \\ -s_{12} c_{23} - c_{12} s_{23} s_{13} e^{i\delta_{13}} & c_{12} c_{23} - s_{12} s_{23} s_{13} e^{i\delta_{13}} & s_{23} c_{13} \\ s_{12} s_{23} - c_{12} c_{23} s_{13} e^{i\delta_{13}} & -c_{12} s_{23} - s_{12} c_{23} s_{13} e^{i\delta_{13}} & c_{23} c_{13} \end{pmatrix} \cdot U_{\text{ph}}, \quad (30)$$

with c_{ij} and s_{ij} stand for $\cos \theta_{ij}$ and $\sin \theta_{ij}$ respectively. In equation (30), the phase matrix is given by:

$$U_{\text{ph}} = \text{diag}(e^{-i\gamma_1}, e^{-i\gamma_2}, 1). \quad (31)$$

where γ_1 and γ_2 are Majorana phases and are chosen in such a way that the elements of M_ν^{diag} are given by

$$M_\nu^{\text{diag}} = \text{diag}(m_1, m_2, m_3), \quad (32)$$

with $m_i, i = 1, 2, 3$, chosen to be real and positive. The Dirac phase δ_{13} is considered for the net charge-parity (CP) violation in lepton number conserving process, where as the Majorana phases γ_1 and γ_2 take part in doubly lepton number violating processes. Once the mixing angles are defined to be in the 1st quadrant, the Dirac phase δ_{13} take values in $[0, 2\pi)$ and the Majorana phases γ_1 and γ_2 can take values between $[0, \pi)$.

A global analysis of the current neutrino oscillation data at 3σ confidence level (C.L.) yields [18]

$$0.25 < \sin^2 \theta_{12} < 0.37, \quad 0.36 < \sin^2 \theta_{23} < 0.67, \quad 0 \leq \sin^2 \theta_{13} < 0.056. \quad (33)$$

While the absolute mass scale of the neutrinos is not yet fixed, the mass square difference have already been determined to a good degree of accuracy:

$$\begin{aligned} \Delta m_o^2 &\equiv m_2^2 - m_1^2 = (7.05 \cdots 8.34) \times 10^{-5} \text{eV}^2 \\ \Delta m_{\text{atm}}^2 &\equiv (m_3^2 - m_1^2) = \pm(2.07 \cdots 2.75) \times 10^{-3} \text{eV}^2. \end{aligned} \quad (34)$$

A crucial issue of neutrino physics is yet to be solved is the mass spectrum which is deeply rooted in the sign of atmospheric mass. That means neutrino mass spectrum could be normal hierarchical (NH) ($m_1 < m_2 < m_3$) or it could be inverted hierarchical (IH) ($m_3 < m_1 < m_2$). Another possibility, yet allowed, is that the neutrino mass spectrum could be degenerate (DG) ($m_1 \sim m_2 \sim m_3$). In any case, cosmology give an upper bound on the sum of the masses of the neutrinos to be [19]

$$\sum_i m_i < 1.3 \text{eV} (95\% \text{C.L.}) \quad (35)$$

In the following we see that it is possible to distinguish NH and IH spectrum of neutrino masses at LHC with a reasonable values of the Yukawa couplings: $f_{\alpha\beta} = (M_\nu)_{\alpha\beta} / \sqrt{2} u_\xi$. However, these couplings can not be too large as they are strongly constrained by the non-observation of lepton flavor violating (LFV) processes. In our case the tree level LFV processes are mainly mediated via the triplet scalar $\xi^{\pm\pm}$ and the one-loop level LFV processes are mediated by $\xi^{\pm\pm}$ and ξ^\pm . Thus for $M_\xi^{\pm\pm}, M_\xi^\pm \lesssim 1 \text{ TeV}$, the spectrum of neutrino masses at LHC can be studied via the decay of $\xi^{\pm\pm}$ and ξ^\pm .

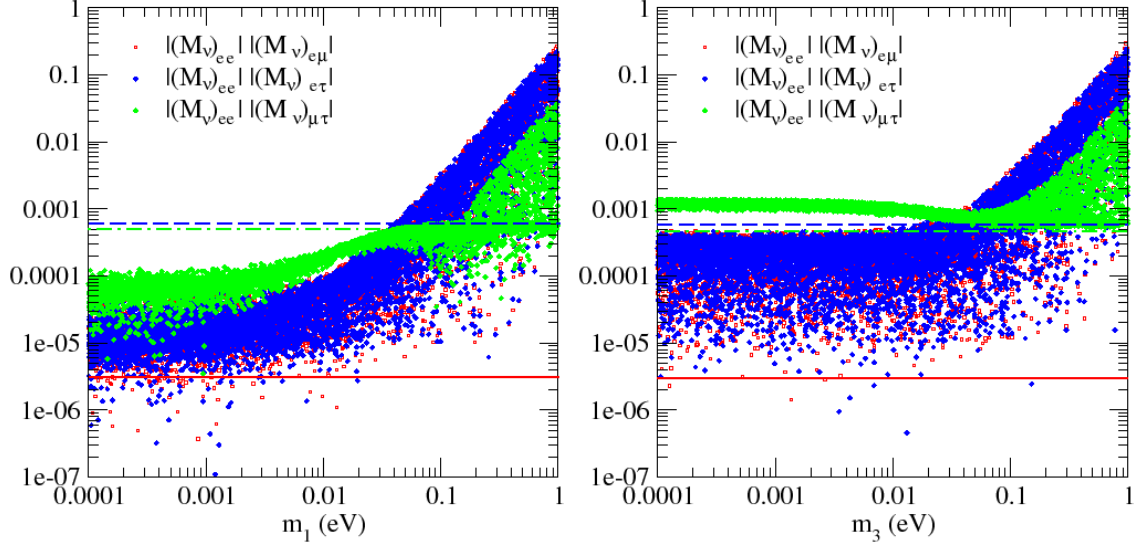


FIG. 2: Scatter plots of $(M_\nu)_{ee}(M_\nu)_{e\mu}$ (red points), $(M_\nu)_{ee}(M_\nu)_{e\tau}$ (blue points) and $(M_\nu)_{ee}(M_\nu)_{e\mu}$ (green points) are shown as a function of lightest neutrino mass for NH (left panel) and IH (right panel), keeping the Majorana phases $\gamma_1 = \gamma_2 = 0$. The LFV constraints on $(M_\nu)_{ee}(M_\nu)_{e\mu}$ (red solid line), $(M_\nu)_{ee}(M_\nu)_{e\tau}$ (blue long-dashed line) and $(M_\nu)_{ee}(M_\nu)_{e\mu}$ (green dot-dashed line) are shown for $M_{\xi\pm\pm} = 500$ GeV and $u_\xi = 1$ eV.

It is almost impossible to constrain the magnitude of individual element of M_ν via the LFV processes since they depend quadratically on the elements of M_ν . The strongest LFV constraint on the elements of M_ν comes from the non-observation of $\mu^- \rightarrow e^- e^+ e^-$. This can be easily checked by estimating the branching fraction:

$$\text{Br}(\mu^- \rightarrow e^- e^+ e^-) \equiv \frac{\Gamma(\mu^- \rightarrow e^- e^+ e^-)}{\Gamma(\mu^- \rightarrow e^- \bar{\nu}_e \nu_\mu)} = \frac{1}{u_\xi^4 G_F^2} \left(\frac{|(M_\nu)_{ee}| |(M_\nu)_{e\mu}|}{M_{\xi^{++}}^2} \right)^2, \quad (36)$$

where $G_F = 1.166 \times 10^{-5}$ GeV⁻² is the Fermi coupling constant. Comparing with the experimental upper bound: $\text{Br}(\mu^- \rightarrow e^- e^+ e^-) < 1.0 \times 10^{-12}$ (at 90% C.L.) [20], we get an upper bound on the neutrino mass matrix elements to be:

$$|(M_\nu)_{ee}| |(M_\nu)_{e\mu}| < 2.9 \times 10^{-6} \text{ eV}^2 \left(\frac{u_\xi}{1 \text{ eV}} \right)^2 \left(\frac{M_{\xi^{++}}}{500 \text{ GeV}} \right)^2. \quad (37)$$

The stringent constraint of $(M_\nu)_{ee}(M_\nu)_{e\mu}$ from $\mu^- \rightarrow e^- e^+ e^-$ can be easily seen from Fig.-2 (see the red solid line), which is shown for $M_{\xi\pm\pm} = 500$ GeV and $u_\xi = 1$ eV. The red data points above that line, allowed by three flavor neutrino oscillation data, are ruled out. The

branching ratios of other tree level LFV processes of the kind $\ell_\alpha \rightarrow \bar{\ell}_\beta \ell_\gamma \ell_\gamma$, but some what less constrained than $\mu^- \rightarrow e^- e^+ e^-$, are given by:

$$\text{Br}(\tau^- \rightarrow e^- e^+ e^-) \equiv \frac{\Gamma(\tau^- \rightarrow e^- e^+ e^-)}{\Gamma(\tau^- \rightarrow \ell_\alpha^- \bar{\nu}_{\ell_\alpha} \nu_\tau)} = \frac{1}{G_F^2 u_\xi^4} \left(\frac{|(M_\nu)_{ee}| |(M_\nu)_{e\tau}|}{M_{\xi^{++}}^2} \right)^2, \quad (38)$$

$$\text{Br}(\tau^- \rightarrow e^- \mu^+ \mu^-) \equiv \frac{\Gamma(\tau^- \rightarrow e^- \mu^+ \mu^-)}{\Gamma(\tau^- \rightarrow \ell_\alpha^- \bar{\nu}_{\ell_\alpha} \nu_\tau)} = \frac{1}{u_\xi^4 G_F^2} \left(\frac{|(M_\nu)_{\mu\mu}| |(M_\nu)_{e\tau}|}{M_{\xi^{++}}^2} \right)^2, \quad (39)$$

$$\text{Br}(\tau^- \rightarrow \mu^- e^+ e^-) \equiv \frac{\Gamma(\tau^- \rightarrow \mu^- e^+ e^-)}{\Gamma(\tau^- \rightarrow \ell_\alpha^- \bar{\nu}_{\ell_\alpha} \nu_\tau)} = \frac{1}{u_\xi^4 G_F^2} \left(\frac{|(M_\nu)_{ee}| |(M_\nu)_{\mu\tau}|}{M_{\xi^{++}}^2} \right)^2, \quad (40)$$

$$\text{Br}(\tau^- \rightarrow \mu^- \mu^+ \mu^-) \equiv \frac{\Gamma(\tau^- \rightarrow \mu^- \mu^+ \mu^-)}{\Gamma(\tau^- \rightarrow \ell_\alpha^- \bar{\nu}_{\ell_\alpha} \nu_\tau)} = \frac{1}{u_\xi^4 G_F^2} \left(\frac{|(M_\nu)_{\mu\mu}| |(M_\nu)_{\mu\tau}|}{M_{\xi^{++}}^2} \right)^2, \quad (41)$$

where $\alpha = e, \mu$. Now comparing the above flavor violating processes with their experimental upper bounds [20]: $\text{Br}(\tau^- \rightarrow e^- e^+ e^-) < 3.6 \times 10^{-8}$ (90% C.L.), $\text{Br}(\tau^- \rightarrow e^- \mu^+ \mu^-) < 3.7 \times 10^{-8}$ (90% C.L.), $\text{Br}(\tau^- \rightarrow \mu^- e^+ e^-) < 2.7 \times 10^{-8}$ (90% C.L.), $\text{Br}(\tau^- \rightarrow \mu^- \mu^+ \mu^-) < 3.2 \times 10^{-8}$ (90% C.L.) we get the following constraints on the elements of (M_ν) :

$$|(M_\nu)_{ee}| |(M_\nu)_{e\tau}| < 5.5 \times 10^{-4} \text{ eV}^2 \left(\frac{u_\xi}{1 \text{ eV}} \right)^2 \left(\frac{M_{\xi^{++}}}{500 \text{ GeV}} \right)^2, \quad (42)$$

$$|(M_\nu)_{\mu\mu}| |(M_\nu)_{e\tau}| < 4.4 \times 10^{-4} \text{ eV}^2 \left(\frac{u_\xi}{1 \text{ eV}} \right)^2 \left(\frac{M_{\xi^{++}}}{500 \text{ GeV}} \right)^2, \quad (43)$$

$$|(M_\nu)_{ee}| |(M_\nu)_{\mu\tau}| < 4.76 \times 10^{-4} \text{ eV}^2 \left(\frac{u_\xi}{1 \text{ eV}} \right)^2 \left(\frac{M_{\xi^{++}}}{500 \text{ GeV}} \right)^2, \quad (44)$$

$$|(M_\nu)_{\mu\mu}| |(M_\nu)_{\mu\tau}| < 5.18 \times 10^{-4} \text{ eV}^2 \left(\frac{u_\xi}{1 \text{ eV}} \right)^2 \left(\frac{M_{\xi^{++}}}{500 \text{ GeV}} \right)^2. \quad (45)$$

At one loop level the LFV processes are mediated by $\xi^{\pm\pm}$ and ξ^\pm . In particular, the concerned processes are $\mu \rightarrow e\gamma$, $\tau \rightarrow e\gamma$ and $\tau \rightarrow \mu\gamma$. The upper bound on $\mu \rightarrow e\gamma$ is given by the MEG Collaboration [21], which reads $\text{Br}(\mu \rightarrow e\gamma) < 1.2 \times 10^{-11}$. On the other hand the estimated branching ratio of $\text{Br}(\mu \rightarrow e\gamma)$ is given by [22, 23]:

$$\text{Br}(\mu \rightarrow e\gamma) \equiv \frac{\Gamma(\mu^- \rightarrow e^- \gamma)}{\Gamma(\mu^- \rightarrow e^- \bar{\nu}_e \nu_\mu)} \approx \frac{27\alpha}{64\pi G_F^2 u_\xi^4} \left(\frac{|(M_\nu^\dagger M_\nu)_{e\mu}|}{M_{\xi^{++}}^2} \right)^2, \quad (46)$$

where $\alpha = e^2/4\pi$, the QED coupling constants. Comparing the above processes with their experimental upper bounds we get the constraint on the elements of neutrino mass matrix to be:

$$|(M_\nu^\dagger M_\nu)_{e\mu}| < 3.2 \times 10^{-4} \text{ eV}^2 \left(\frac{u_\xi}{1 \text{ eV}} \right)^2 \left(\frac{M_{\xi^{++}}}{500 \text{ GeV}} \right)^2. \quad (47)$$

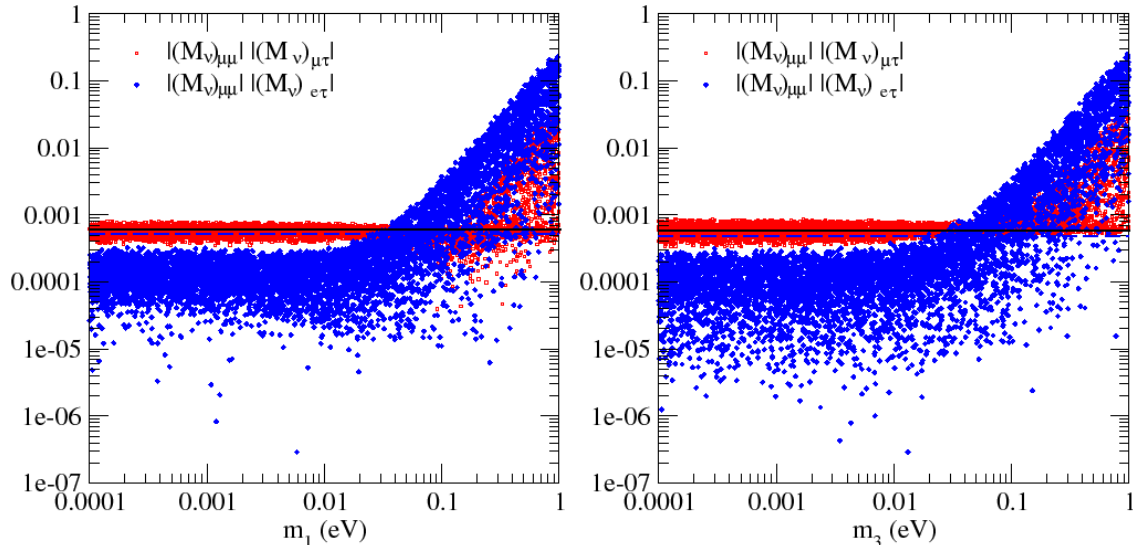


FIG. 3: Scatter plots of $(M_\nu)_{\mu\mu}(M_\nu)_{\mu\tau}$ (red points) and $(M_\nu)_{\mu\mu}(M_\nu)_{e\tau}$ (blue points) are shown as a function of lightest neutrino mass for NH (left panel) and IH (right panel), keeping the Majorana phases $\gamma_1 = \gamma_2 = 0$. The LFV constraints on $(M_\nu)_{\mu\mu}(M_\nu)_{\mu\tau}$ (black solid line) and $(M_\nu)_{\mu\mu}(M_\nu)_{e\tau}$ (blue dashed line) are shown for $M_{\xi^{\pm\pm}} = 500$ GeV and $u_\xi = 1$ eV.

Similarly the constraints on $(M_\nu^\dagger M_\nu)_{e\tau}$ and $(M_\nu^\dagger M_\nu)_{\mu\tau}$ can be obtained as follows:

$$|(M_\nu^\dagger M_\nu)_{e\tau}| < 3.07 \times 10^{-2} \left(\frac{M_{\xi^{++}}}{500\text{GeV}} \right)^2, \quad (48)$$

$$|(M_\nu^\dagger M_\nu)_{\mu\tau}| < 1.96 \times 10^{-3} \left(\frac{M_{\xi^{++}}}{500\text{GeV}} \right)^2. \quad (49)$$

V. PRODUCTION AND DECAY OF $\xi^{\pm\pm}$

The triplet scalar appears in several extensions of the SM. There exist many extensive discussions on the collider search of this triplet scalar for various models at LEP, Tevatron and LHC [12, 24–30]. Here we discuss the same sign dilepton signature of triplet scalars in presence of an extra Z_{B-L} gauge boson [31]. Our analysis is based on the parton-level simulation. However, we have not included any QCD corrections [32] which may enhance the cross-sections by 20% - 30%.

As discussed in section-III, the low energy effective theory of our model contains not only a TeV scale $B - L$ gauge boson, but also a pair of doubly charged scalars: $\xi^{\pm\pm}$ of

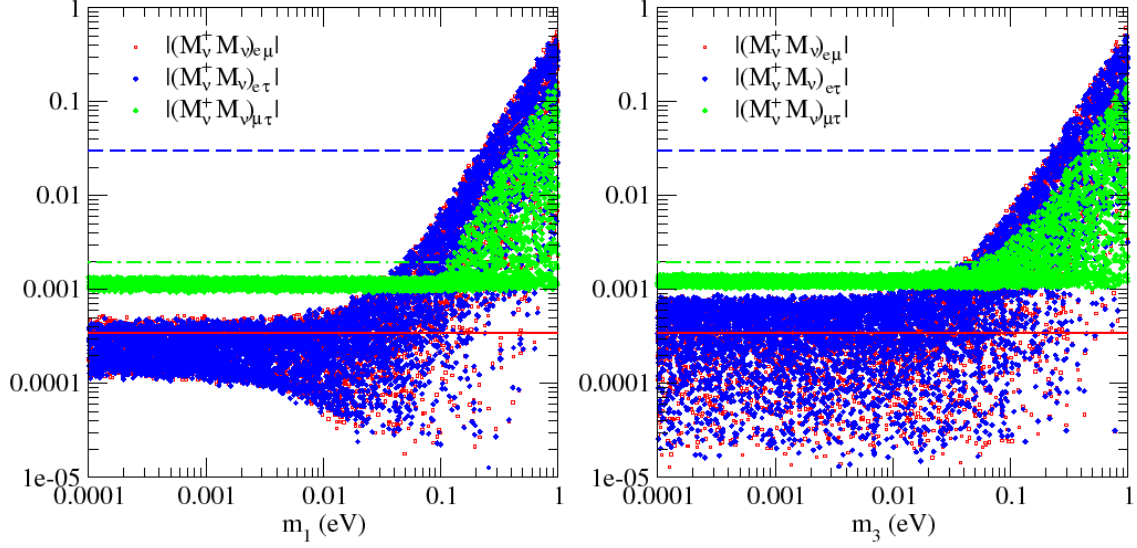


FIG. 4: Scatter plots of $(M_\nu^\dagger M_\nu)_{e\mu}$ (red points), $(M_\nu^\dagger M_\nu)_{e\tau}$ (blue points) and $(M_\nu^\dagger M_\nu)_{\mu\tau}$ (green points) are shown as a function of lightest neutrino mass for NH (left panel) and IH (right panel), keeping the Majorana phases $\gamma_1 = \gamma_2 = 0$. The LFV constraints on $(M_\nu^\dagger M_\nu)_{e\mu}$ (red solid line), $(M_\nu^\dagger M_\nu)_{e\tau}$ (blue dashed line) and $(M_\nu^\dagger M_\nu)_{\mu\tau}$ (green dot dashed line) are shown for $M_{\xi^{\pm\pm}} = 500$ GeV and $u_\xi = 1$ eV.

mass $M_{\xi^{\pm\pm}} \lesssim 1$ TeV. Therefore, depending on the relative magnitude between $M_{Z_{B-L}}$ and $M_{\xi^{\pm\pm}}$, the production cross-section of $\xi^{\pm\pm}$ will vary. In particular, if $M_{Z_{B-L}} > 2M_{\xi^{\pm\pm}}$, then at LHC $\xi^{\pm\pm}$ particles can be pair produced via Z_{B-L} decay since the branching fraction of $Z_{B-L} \rightarrow \xi^{\pm\pm}\xi^{\mp\mp}$ is not negligible. On the other hand, if $M_{Z_{B-L}} < 2M_{\xi^{\pm\pm}}$, then at LHC $\xi^{\pm\pm}$ particles can be produced via Drell-Yan process. In such a case we discuss the parton level process: $q\bar{q}' \rightarrow \xi^{\pm\pm}\xi^{\mp\mp}$ mediated by Z^* , γ^* and Z_{B-L}^* . The differential cross-section⁶ for this process is given by:

$$\frac{d\sigma}{dt}(q\bar{q}' \rightarrow \xi^{\pm\pm}\xi^{\mp\mp}) = \frac{\pi\alpha^2}{3\hat{s}^2}\mathcal{M}^2, \quad (50)$$

where the \mathcal{M}^2 is given by

$$\begin{aligned} \mathcal{M}^2 = & \left\{ \mathcal{M}_\gamma^2 + \mathcal{M}_Z^2 + \mathcal{M}_{\gamma-Z}^2 + (4\pi\alpha)^{-2} \left(\mathcal{M}_{Z_{B-L}}^2 + 4\pi\alpha \left[\mathcal{M}_{\gamma-Z_{B-L}}^2 + \mathcal{M}_{Z-Z_{B-L}}^2 \right] \right) \right\} \\ & \times \left[(\hat{t} - M_{\xi^{++}}^2)^2 + \hat{s}\hat{t} \right]. \end{aligned} \quad (51)$$

⁶ We have neglected a small contribution that may appear from the two photon channel [33].

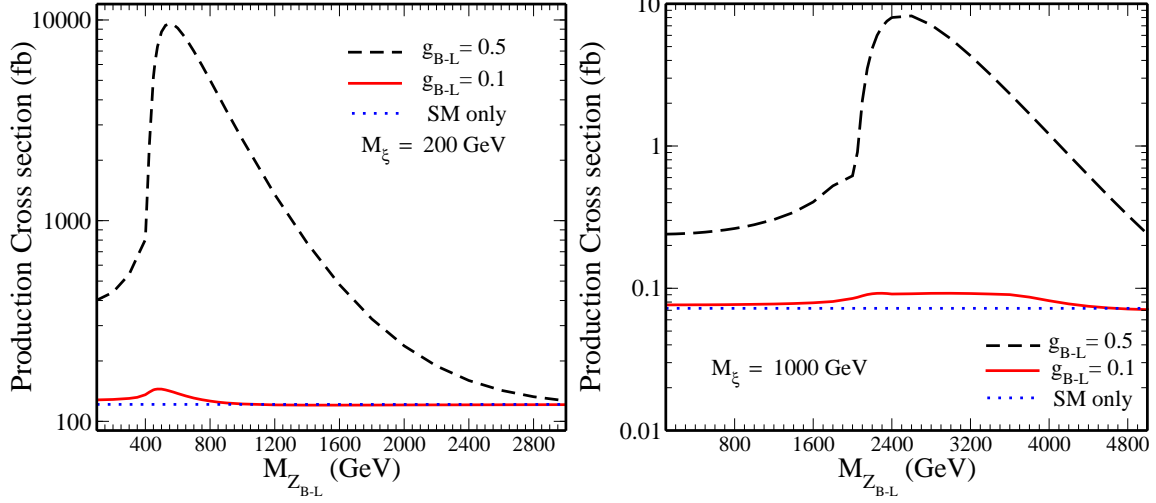


FIG. 5: The Drell-Yan production cross-section of $\xi^{\pm\pm}$ at LHC is shown as a function of $M_{Z_{B-L}}$ with center of mass energy 14 TeV for $g_{B-L} = 0.1$ (solid red-line) and $g_{B-L} = 0.5$ (dashed black-line) at $M_{\xi^{\pm\pm}} = 200$ GeV (left-panel) and $M_{\xi^{\pm\pm}} = 1$ TeV (right-panel). The SM contribution, which is independent of Z_{B-L} , is shown by a horizontally-flat dotted line (Blue).

In the Eqs. (50) and (51) \hat{s}, \hat{t} are the parton level Mandelstam variables and α is the QED coupling constant. Different \mathcal{M}^2 in Eq. (51) can be read as

$$\begin{aligned}
\mathcal{M}_\gamma^2 &= -\frac{2Q_\xi^2 Q_q^2}{\hat{s}^2} \\
\mathcal{M}_Z^2 &= -\frac{(1 + X_q^2)}{8 [(\hat{s} - M_Z^2)^2 + \Gamma_Z^2 M_Z^2]} \left(\frac{1 - 2 \sin^2 \theta_W}{\sin^2 \theta_W \cos^2 \theta_W} \right)^2 \\
\mathcal{M}_{\gamma-Z}^2 &= -\frac{Q_\xi Q_q X_q (\hat{s} - M_Z^2)}{\hat{s} [(\hat{s} - M_Z^2)^2 + \Gamma_Z^2 M_Z^2]} \left(\frac{1 - 2 \sin^2 \theta_W}{\sin^2 \theta_W \cos^2 \theta_W} \right) \\
\mathcal{M}_{Z_{B-L}}^2 &= -\frac{2g_{B-L}^4 (Y_{B-L}^q Y_{B-L}^\xi)^2}{(\hat{s} - M_{Z_{B-L}}^2)^2 + \Gamma_{Z_{B-L}}^2 M_{Z_{B-L}}^2} \\
\mathcal{M}_{\gamma-Z_{B-L}}^2 &= -\frac{4Q_\xi g_{B-L}^2 Q_q Y_{B-L}^q Y_{B-L}^\xi (\hat{s} - M_{Z_{B-L}}^2)}{\hat{s} [(\hat{s} - M_{Z_{B-L}}^2)^2 + \Gamma_{Z_{B-L}}^2 M_{Z_{B-L}}^2]} \\
\mathcal{M}_{Z-Z_{B-L}}^2 &= -\frac{2g_{B-L}^2 X_q Y_{B-L}^q Y_{B-L}^\xi [(\hat{s} - M_Z^2)(\hat{s} - M_{Z_{B-L}}^2) - \Gamma_Z \Gamma_{Z_{B-L}} M_Z M_{Z_{B-L}}]}{[(\hat{s} - M_Z^2)^2 + \Gamma_Z^2 M_Z^2] [(\hat{s} - M_{Z_{B-L}}^2)^2 + \Gamma_{Z_{B-L}}^2 M_{Z_{B-L}}^2]}. \quad (52)
\end{aligned}$$

Here $Q_\xi = 2$, $Q_q = 2/3$, $X_q = 1 - (8/3) \sin^2 \theta_W$ for up-type quarks and $Q_q = -1/3$, $X_q = -1 + (4/3) \sin^2 \theta_W$ for down-type quarks, while Y_{B-L}^ξ and Y_{B-L}^q are the B-L quantum numbers of the ξ -scalar and quark respectively.

The Drell-Yan production cross-section of $\xi^{\pm\pm}$ at LHC mediated by γ , Z and

Z_{B-L} gauge bosons are shown in Fig.-5 by taking $B - L$ gauge boson decay width: $\Gamma_{Z_{B-L}} = 0.03M_{Z_{B-L}}$. For illustration purpose we have shown the production cross-section of $\xi^{\pm\pm}$ for $g_{B-L} = 0.1, 0.5$ and $M_{\xi^{\pm\pm}} = 200 \text{ GeV}, 1 \text{ TeV}$. We have used CTEQ6 [34] for the parton level distribution function with the factorization scale is set as the partonic center of mass (c.m.) energy ($\sqrt{\hat{s}}$). From Fig.-5 we see that the production cross-section of $\xi^{\pm\pm}$ at resonance ($\hat{s} \sim M_{Z_{B-L}}^2$) is significantly larger than the SM contribution (dotted-blue line), which is independent of $M_{Z_{B-L}}$. However, we note that this enhancement strongly depends on the magnitude of g_{B-L} . This can be easily checked from the amplitude square: $\mathcal{M}_{Z_{B-L}}^2$, which varies as g_{B-L}^4 . Recall that for $g_{B-L} > 0.1(0.5)$, the current experimental constraint on Z_{B-L} mass, given by Eq. (26), gives $M_{Z_{B-L}} > 600 \text{ GeV}$ ($M_{Z_{B-L}} > 3 \text{ TeV}$). Thus for $M_{\xi^{\pm\pm}} = 200 \text{ GeV}$, as shown in the left-panel of Fig. (5), we see that at $g_{B-L} \geq 0.1$ ($g_{B-L} \geq 0.5$) and $M_{Z_{B-L}} \geq 600 \text{ GeV}$ ($M_{Z_{B-L}} = 3 \text{ TeV}$), the total production cross-section of $\xi^{\pm\pm}$ due to the presence of Z_{B-L} enhances by 14.7% (4.6%) with respect to the SM contribution. On the other hand, for $M_{\xi^{\pm\pm}} = 1 \text{ TeV}$, as shown in the right-panel of Fig. (5), we see that at $g_{B-L} \geq 0.1$ ($g_{B-L} \geq 0.5$) and $M_{Z_{B-L}} \geq 600 \text{ GeV}$ ($M_{Z_{B-L}} = 3 \text{ TeV}$), the off-shell contribution of Z_{B-L} to the production of $\xi^{\pm\pm}$ dominates over the SM contribution. This can be easily seen from Fig.-6, where we have shown the variation of the production cross-section as a function of $M_{\xi^{\pm\pm}}$ at different values of $M_{Z_{B-L}}$. In all the cases the cross-section drops quickly with the increase of the charged scalar mass, as it is expected. However, for large $M_{Z_{B-L}}$, the resonance occurs for higher values of $M_{\xi^{\pm\pm}}$ and hence the Z_{B-L} contribution drops slowly than the SM contribution. Our estimation shows that at $M_{\xi^{++}} = 300 \text{ GeV}$, for $g_{B-L} = 0.1$ and $M_{Z_{B-L}} = 700 \text{ GeV}$, the number of expected events (cross-section \times Luminosity), at LHC with an integrated luminosity of 30fb^{-1} , is 200, 450 and 900 respectively at center of mass energy 7 TeV, 10 TeV and 14 TeV.

A. Decay of $\xi^{\pm\pm}$

Once the $\xi^{\pm\pm}$ particles are produced, they decay to SM particles. The decay channels of $\xi^{\pm\pm}$ can be studied at LHC for $M_{\xi^{\pm\pm}} \lesssim 1 \text{ TeV}$ with an integrated luminosity $\gtrsim 30\text{fb}^{-1}$. A ξ^{++} can decay either to two like-sign charged leptons ($l_\alpha^+ l_\beta^+$, $\alpha, \beta = e, \mu, \tau$) or to W^+W^+ . It can also decay to $W^+\xi^+$. However, the decay rate of $\xi^{++} \rightarrow W^+\xi^+$ is phase space suppressed

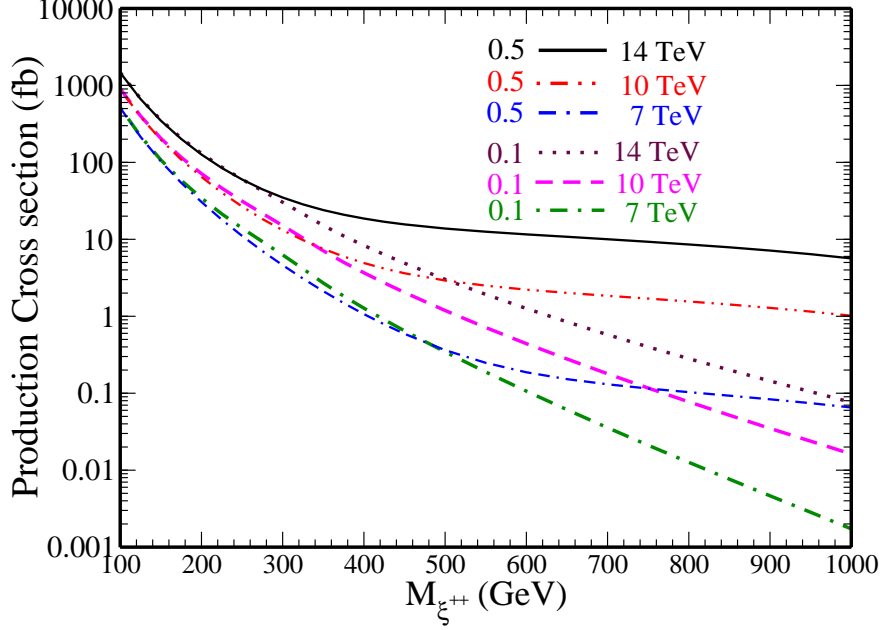


FIG. 6: The Drell-Yan production cross-section of $\xi^{\pm\pm}$ at LHC is shown as a function of $M_{\xi^{\pm\pm}}$ for $g_{B-L} = 0.5$ and $M_{Z_{B-L}} = 3$ TeV with center of mass energy 14 TeV (solid black line), 10 TeV (double dot-dashed red line) and 7 TeV (double dash-dotted blue line). The same is also shown for $g_{B-L} = 0.1$ and $M_{Z_{B-L}} = 700$ GeV at center of mass energy: 14 TeV (dotted maroon line) 10 TeV (dashed magenta line) and 7 TeV (dot-dashed green line).

as the mass of ξ^+ is of the similar order of $M_{\xi^{++}}$. Therefore, in what follows we will consider only the decay of ξ^{++} in the former two channels. The corresponding partial decay widths can be given as:

$$\Gamma(\xi^{++} \rightarrow l_{\alpha}^{+} l_{\beta}^{+}) = \frac{M_{\xi^{++}}}{4\pi u_{\xi}^2 (1 + \delta_{\alpha\beta})} |(M_{\nu})_{\alpha\beta}|^2 \quad (53)$$

and

$$\Gamma(\xi^{++} \rightarrow W^{+} W^{+}) = \frac{g^4 u_{\xi}^2 M_{\xi^{++}}^3}{32\pi M_W^4} \left[1 - 4 \left(\frac{M_W}{M_{\xi^{++}}} \right)^2 \right]^{1/2} \left[1 - 4 \left(\frac{M_W}{M_{\xi^{++}}} \right)^2 + 12 \left(\frac{M_W}{M_{\xi^{++}}} \right)^4 \right], \quad (54)$$

where $\delta_{\alpha\beta}$ is the Kronecker delta. From Eqs. (53) and (54) we see that the decay rate of ξ^{++} depends not only on its mass, but also on the vev u_{ξ} . For small u_{ξ} , $\Gamma(\xi^{++} \rightarrow l_{\alpha}^{+} l_{\beta}^{+})$ dominates since it varies inversely with u_{ξ}^2 , while for large u_{ξ} , $\Gamma(\xi^{++} \rightarrow W^{+} W^{+})$ dominates as it varies directly with u_{ξ}^2 . This can be easily seen from the right panel of Fig.-7, where

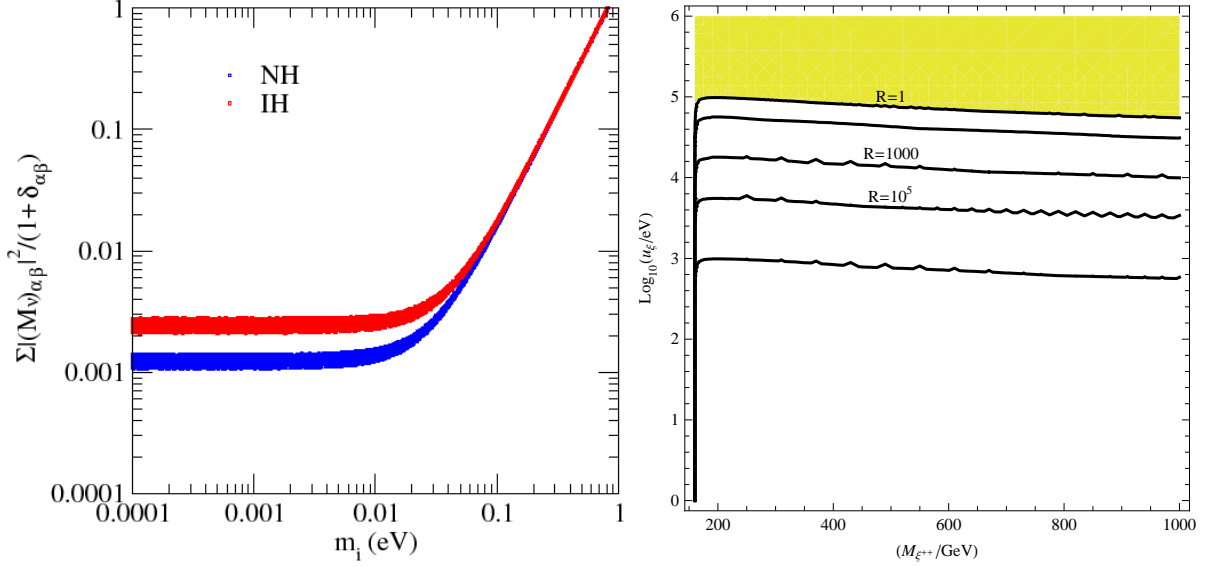


FIG. 7: The variation of $\sum_{\alpha,\beta} |(M_\nu)_{\alpha,\beta}|^2/(1 + \delta_{\alpha\beta})$ with respect to the lightest neutrino mass ($i=1$ (NH) and $i=3$ (IH)), keeping the Majorana phases $\gamma_1 = \gamma_2 = 0$, is shown on the left panel, while the contours of R in the plane of $M_{\xi^{++}}$ versus u_ξ are shown on the right panel. In the shaded region (right panel) $R < 1$ and hence ξ^{++} decays dominantly to W^+W^+ .

we have shown the contours of the ratio:

$$R = \frac{\Gamma(\xi^{++} \rightarrow l_\alpha^+ l_\beta^+)}{\Gamma(\xi^{++} \rightarrow W^+ W^+)} . \quad (55)$$

for a typical value of $\sum_{\alpha,\beta} |(M_\nu)_{\alpha,\beta}|^2/(1 + \delta_{\alpha\beta}) = 3 \times 10^{-3}$. However, from the left panel of Fig.-7 we infer that the value of $\sum_{\alpha,\beta} |(M_\nu)_{\alpha,\beta}|^2/(1 + \delta_{\alpha\beta})$ does not change significantly for $m_i < 0.1$ eV, with $i=1$ (NH) and $i=3$ (IH)). In other words, the value of R is almost independent of the hierarchy of neutrino masses. In either case (NH or IH), for $u_\xi < 10^5$ eV, the decay of ξ^{++} is leptophilic and hence dominantly decays to two leptons of same sign. The like-sign dilepton channel of ξ^{++} is almost background free and can be seen without mistaken at LHC for $M_{\xi^{++}} \lesssim 1$ TeV. The mass of ξ^{++} is approximately about the invariant mass of the two like sign leptons.

By studying the dilepton signal of ξ^{++} the nature of neutrino mass spectrum (NH or IH) can be resolved. A $\xi^{\pm\pm}$ can simultaneously decay to $e^\pm e^\pm$, $\mu^\pm \mu^\pm$, $\tau^\pm \tau^\pm$, $e^\pm \mu^\pm$, $e^\pm \tau^\pm$ and $\mu^\pm \tau^\pm$ with different strengths depending on the magnitude of $(M_\nu)_{\alpha\beta}$, $\alpha, \beta = e, \mu, \tau$. However, the decay of $\xi^{\pm\pm}$ to $\tau^\pm \tau^\pm$, $e^\pm \tau^\pm$ and $\mu^\pm \tau^\pm$ can be misguided at collider since the muons coming out from τ decay can have similar momentum distribution as that of

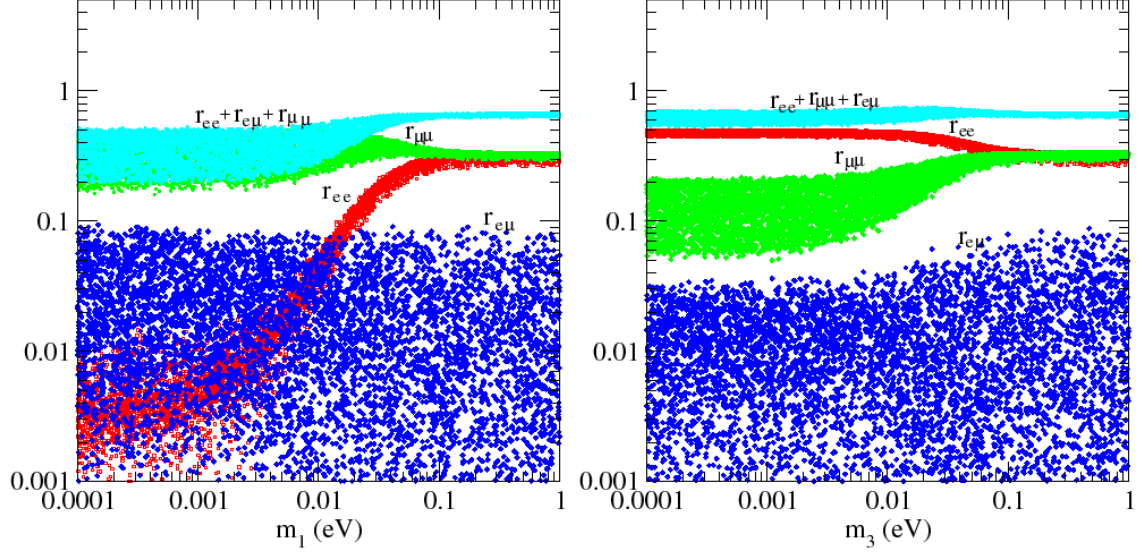


FIG. 8: Branching ratios: r_{ee} (red points), $r_{e\mu}$ (blue points), $r_{\mu\mu}$ (green points) and $r_{ee} + r_{e\mu} + r_{\mu\mu}$ (cyan points) for NH (left panel) and IH (right panel) are shown against the lightest neutrino mass keeping Majorana phases $\gamma_1 = \gamma_2 = 0$.

muons coming out from $\xi^{\pm\pm}$. Therefore, in what follows we focus only the signature of $\xi^{\pm\pm}$ through its decay to $e^\pm e^\pm$, $\mu^\pm \mu^\pm$ and $e^\pm \mu^\pm$. In order to study the decay of $\xi^{\pm\pm}$ through these channels we define the branching fractions:

$$\begin{aligned}
 r_{ee} &\equiv \text{Br}(\xi^{\pm\pm} \rightarrow e^\pm e^\pm) = \frac{\Gamma(\xi^{\pm\pm} \rightarrow e^\pm e^\pm)}{\sum_{\alpha\beta} \Gamma(\xi^{\pm\pm} \rightarrow \ell_\alpha^\pm \ell_\beta^\pm)} \\
 r_{\mu\mu} &\equiv \text{Br}(\xi^{\pm\pm} \rightarrow \mu^\pm \mu^\pm) = \frac{\Gamma(\xi^{\pm\pm} \rightarrow \mu^\pm \mu^\pm)}{\sum_{\alpha\beta} \Gamma(\xi^{\pm\pm} \rightarrow \ell_\alpha^\pm \ell_\beta^\pm)} \\
 r_{e\mu} &\equiv \text{Br}(\xi^{\pm\pm} \rightarrow e^\pm \mu^\pm) = \frac{\Gamma(\xi^{\pm\pm} \rightarrow e^\pm \mu^\pm)}{\sum_{\alpha\beta} \Gamma(\xi^{\pm\pm} \rightarrow \ell_\alpha^\pm \ell_\beta^\pm)}
 \end{aligned} \tag{56}$$

where $\alpha, \beta = e, \mu, \tau$. The branching ratios are shown in Fig.-8. It can be seen from there that in case of NH with $m_1 \ll 0.1$ eV, the decays of $\xi^{\pm\pm}$ to $\mu^\pm \mu^\pm$ is 20 to 50 percent while the decay of $\xi^{\pm\pm}$ to $e^\pm \mu^\pm$ is less than 10 percent and to $e^\pm e^\pm$ is less than a percent. On the other hand, in case of inverted hierarchy with $m_3 \ll 0.1$ eV, the decay of $\xi^{\pm\pm}$ to $e^\pm e^\pm$ is about 40 to 50 percent and to $\mu^\pm \mu^\pm$ is less than 20 percent while its decays to $e^\pm \mu^\pm$ is almost negligible. Thus the sum of $r_{ee} + r_{e\mu} + r_{\mu\mu}$ is 20 to 40 percent in case of NH, while it is 50 to 70 percent in case of IH. This is the striking feature for distinguishing NH from IH at collider.

Even though we argued that the decay of $\xi^{\pm\pm}$ is background free, it is not necessarily

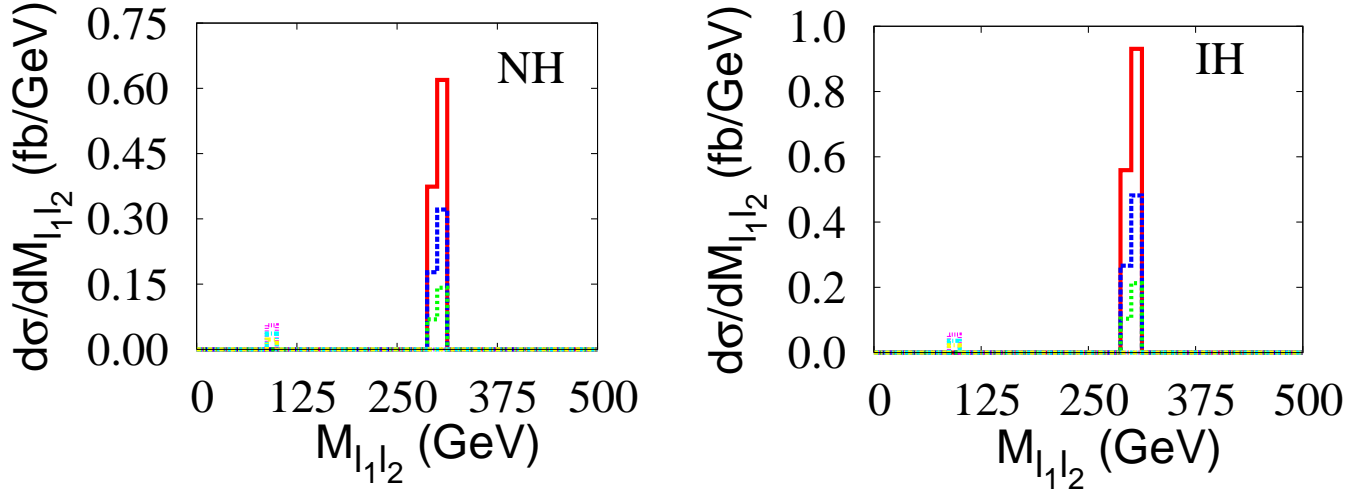


FIG. 9: The Differential cross section versus the invariant mass at center of mass energy 7 TeV (green), 10 TeV (blue) and 14 TeV (red) with $g_{B-L} = 0.1$ and $M_{Z_{B-L}} = 700$ GeV. We set $r_{ee} + r_{\mu\mu} + r_{e\mu}$ to be 40% for NH (left panel) and 60% for IH (right panel).

true. The small SM background will appear from the two Z-boson decay. We have estimated the parton level SM background using MADGRAPH [35] and CTEQ6. The differential scattering cross section are plotted as a function of the two like-sign charged leptons invariant mass $M_{l_1 l_2}$. Both the like-sign charged lepton invariant masses, coming from two SM Z-decay or the doubly charged scalar decay, are shown in the Fig.-9 for three different values of the c.m energy. The like-sign dileptons appearing from the doubly-charged scalar decay will show a peak at it's mass and are shown at c.m. energy 7 TeV (green, dotted), 10 TeV (blue, dashed) and 14 TeV (red, solid). On the other hand, a very small background from two Z-boson decay will show up at M_Z . We have used a minimal cut off $p_T^{l_i} > 5$ GeV for both signal and background. In addition, to remove any possible background of lepton pairs produced from photons we have incorporated $M_{l_1 l_2} > 5$ GeV and also ΔR -isolation of 0.12 between each pair of leptons (where the angular separation, $\Delta R = \sqrt{(\Delta\eta)^2 + (\Delta\phi)^2}$). Since the signal and background dilepton peaks are well separated from each other, so with the use of a cut $|M_{l_1 l_2} - M_z| > 5\text{GeV}$, we can remove this background without any ambiguity. From Fig.-8 we see that the $r_{ee} + r_{e\mu} + r_{\mu\mu}$ is 40% in case of normal hierarchy while it is 60% in case of inverted hierarchy. Using this in Fig.-9, we have shown the invariant mass

distribution for NH (IH) in the left (right) panel. One important message from Fig.-9 is that the differential cross-section, hence the number of events, in case of NH is reasonably less than the corresponding value in case of IH. For example, with 14 TeV c.m. energy the number of expected events are 540 (360) for IH (NH). This criteria can be used to distinguish the NH spectrum from the IH spectrum of neutrino masses.

VI. PRODUCTION AND DECAY OF ξ^\pm

Before going to conclusion let us briefly discuss about the signature of singly charged scalar particles ξ^\pm . The ξ^\pm can be produced along with the doubly charged scalars ($\xi^{\mp\mp}$) through the Drell-Yan process: $q\bar{q}' \rightarrow \xi^{\mp\mp}\xi^\pm$ mediated via the charged weak gauge boson $W^{\pm*}$. Moreover, ξ^\pm can also be pair produced through the Drell-Yan process: $q\bar{q} \rightarrow \xi^\pm\xi^\mp$ mediated by Z^* , γ^* and Z_{B-L} , the same way as the doubly charged scalar particles are produced. Hence the decay of these particles can be studied at LHC.

Once the ξ^\pm particles are produced, they decay dominantly through the channel: $\xi^+ \rightarrow \ell^+ + \nu$. Since the neutrinos are invisible at detector, the decay of ξ^\pm , produced through the channel $q\bar{q}' \rightarrow \xi^{\pm\pm}\xi^\mp$ mediated via the the charged weak gauge boson $W^{\pm*}$, will lead to a three lepton final state: $\ell^\pm\ell^\pm\ell^\mp$. On the other hand, the decay of ξ^\pm , produced through the channel $q\bar{q}' \rightarrow \xi^\pm\xi^\mp$ mediated by Z^* , γ^* and Z_{B-L}^* , will lead to a two lepton final state: $\ell^\pm\ell^\mp$. In either case, we have large SM background. However, with a proper selection of cuts one can study these events at LHC [30].

VII. CONCLUSION

In this article, we proposed a variant of type-II seesaw to generate the sub-eV neutrino masses. The seesaw is realized at the TeV scale, while retaining the philosophy of seesaw intact. It is executed in a gauged $U(1)_{B-L}$ symmetric model by introducing two $SU(2)_L$ triplet scalars Δ and ξ with B-L quantum number 0 and 2 respectively. The triplet scalar Δ is assumed to be super heavy, while the mass of ξ is at the TeV scale. However, we showed that they equally contribute to the neutrino masses even though their masses differ by several orders of magnitude. This could be achieved due to a small mixing between Δ and ξ , which arises at the TeV scale via the breaking of $U(1)_{B-L}$ symmetry. Note that the

small mixing is required to realism the seesaw at TeV scale. Since Δ is super heavy and its mixing with ξ is very small, it gets decoupled from the low energy effective theory. As a result, in the low energy effective theory, the only doubly and singly charged scalars appear are $\xi^{\pm\pm}$ and ξ^\pm . In other words, the number of degrees of freedom in the effective theory is exactly same as that of "original type-II seesaw" or its variant "triplet scalar model", apart from a B-L gauge boson. Therefore, it is worth mentioning the following distinctive features of the model:-

- The low energy effective theory not only have doubly charged scalars, but also have a Z_{B-L} gauge boson whose signature at collider can be studied.
- If $M_{Z_{B-L}} < 2M_{\xi^{\pm\pm}}$ mass then the Z_{B-L} boson enhances the production cross-section of doubly charged scalars via Drell-Yan process.
- If $M_{Z_{B-L}} > 2M_{\xi^{\pm\pm}}$ then the on-shell decay of Z_{B-L} to $\xi^{\pm\pm}\xi^{\mp\mp}$ can populate doubly charged scalars at collider.

Since the mass of $\xi^{\pm\pm}$ is at the TeV scale, it can be pair produced at LHC via the Drell-Yan process. For $\langle\xi\rangle < 10^5$ eV, the $\xi^{\pm\pm}$ is leptophilic and dominantly decays to two leptons of same sign. This signature of $\xi^{\pm\pm}$ is almost free of SM background. For example, we found that by taking $M_{\xi^{++}} = 300$ GeV, $g_{B-L} = 0.1$, $M_{Z_{B-L}} = 700$ GeV and with an integrated luminosity of 30fb^{-1} , the number expected events are 200, 450 and 900 at c.m energy 7 TeV, 10 TeV and 14 TeV respectively. By studying the decay of $\xi^{\pm\pm} \rightarrow \ell^\pm\ell^\pm$ the nature of hierarchy (NH or IH) can be resolved at LHC. We have considered the decay channel of $\xi^{\pm\pm}$ involving e and μ only. It is shown that in case of NH, the branching ratio of the decay of $\xi^{\pm\pm} \rightarrow e^\pm e^\pm + \mu^\pm\mu^\pm + e^\pm\mu^\pm$ is about 20 to 50 percent, while in case of IH it is about 50 to 70 percent. So, one could expect more number of events in case of IH than NH. This conclusion is obtained by setting the Majorana phases to zero.

The singly charged scalars ξ^\pm can also be pair produced via the Drell-Yan process at LHC. The ξ^\pm particles then dominantly decay to charged leptons and neutrinos. Since neutrinos are invisible, the number of final state leptons in this case is two. On the other hand, ξ^\pm can also be produced along with the doubly charged scalars and hence lead to a trilepton final state. In either case, the SM background is significantly large. However, it is possible to study these events by proper selection of cuts.

Acknowledgement

Authors would like to thank Jean-Marc Gérard, Fabio Maltoni, Utpal Sarkar, Ernest Ma and Jean-Marie Frère, Maria Kadastik and Tao Han for useful discussions. The work of SKM is partially supported by the Belgian Federal Office for Scientific, Technical and Cultural Affairs through the Inter-university Attraction Pole No. P6/11. The work of NS is partially supported by IISN and the Belgian Science Policy (IAP VI-11).

- [1] S. Weinberg, *Phys. Rev. Lett.* **43**, 1566, 1979 .
- [2] E. Ma, *Phys. Rev. Lett.* **81**, 1171 (1998) [arXiv:hep-ph/9805219].
- [3] P. Minkowski, *Phys. Lett. B* **67** (1977) 421; M. Gell-Mann, P. Ramond and R. Slansky, *Proceedings of the Supergravity Stony Brook Workshop*, eds. P. van Nieuwenhuizen and D. Freedman (New York, 1979); T. Yanagida, *Proceedings of the Workshop on the Baryon Number of the Universe and Unified Theories*, Tsukuba, Japan, 13-14 Feb 1979; R. N. Mohapatra and G. Senjanovic, *Phys. Rev. Lett.* **44**, 912 (1980) .
- [4] K. S. Babu, S. Nandi and Z. Tavartkiladze, *Phys. Rev. D* **80**, 071702 (2009) [arXiv:0905.2710 [hep-ph]]; F. Bonnet, D. Hernandez, T. Ota and W. Winter, *JHEP* **0910**, 076 (2009) [arXiv:0907.3143 [hep-ph]]; I. Gogoladze, N. Okada and Q. Shafi, *Phys. Lett. B* **672**, 235 (2009) [arXiv:0809.0703 [hep-ph]].
- [5] I. Picek and B. Radovic, arXiv:0911.1374 [hep-ph].
- [6] R.N. Mohapatra, *Phys. Rev. Lett.* **56** (1986), p. 61. R.N. Mohapatra and J.W.F. Valle, *Phys. Rev. D* **34**, 1642 (1986).
- [7] D. Cogollo, H. Diniz and C. A. d. Pires, arXiv:1002.1944 [hep-ph].
- [8] R. Foot, H. Lew, X. G. He and G. C. Joshi, *Z. Phys. C* **44**, 441 (1989); E. Ma, *Phys. Rev. Lett.* **81**, 1171 (1998) [hep-ph/9805219] .
- [9] R. Franceschini, T. Hambye and A. Strumia, *Phys. Rev. D* **78**, 033002 (2008) [arXiv:0805.1613 [hep-ph]].
- [10] M. Magg and C. Wetterich, *Phys. Lett. B* **94**, 61 (1980); T. P. Cheng and L. F. Li, *Phys. Rev. D* **22**, 2860 (1980); G. B. Gelmini and M. Roncadelli, *Phys. Lett. B* **99**, 411 (1981); G. Lazarides, Q. Shafi and C. Wetterich, *Nucl. Phys. B* **181**, 287 (1981) ; R. N. Mohapatra

- and G. Senjanovic, Phys. Rev. D **23**, 165 (1981); J.Schechter and J.W.F. Valle, Phys. Rev. D. **22**, 2227, (1980).
- [11] E. Ma and U. Sarkar, Phys. Rev. Lett. **80**, 5716 (1998) [arXiv:hep-ph/9802445].
- [12] A. G. Akeroyd, M. Aoki and H. Sugiyama, Phys. Rev. D **77**, 075010 (2008) [arXiv:0712.4019 [hep-ph]]; J. Garayoa and T. Schwetz, JHEP **0803**, 009 (2008) [arXiv:0712.1453 [hep-ph]]; E. J. Chun, K. Y. Lee and S. C. Park, Phys. Lett. B **566**, 142 (2003) [arXiv:hep-ph/0304069]; M. Kadastik, M. Raidal and L. Rebane, Phys. Rev. D **77**, 115023 (2008) [arXiv:0712.3912 [hep-ph]]; P. Fileviez Perez, T. Han, G. y. Huang, T. Li and K. Wang, Phys. Rev. D **78**, 015018 (2008) [arXiv:0805.3536 [hep-ph]].
- [13] J. McDonald, N. Sahu and U. Sarkar, JCAP **0804**, 037 (2008) [arXiv:0711.4820 [hep-ph]]; N. Sahu and U. Sarkar, Phys. Rev. D **76**, 045014 (2007) [arXiv:hep-ph/0701062].
- [14] E. Ma, Phys. Rev. Lett. **86**, 2502 (2001) [arXiv:hep-ph/0011121]; W. Chao, Z. g. Si, Y. j. Zheng and S. Zhou, Phys. Lett. B **683**, 26 (2010) [arXiv:0907.0935 [hep-ph]]; N. Haba, S. Matsumoto and K. Yoshioka, Phys. Lett. B **677**, 291 (2009) [arXiv:0901.4596 [hep-ph]]; S. K. Majee, M. K. Parida and A. Raychaudhuri, Phys. Lett. B **668**, 299 (2008) [arXiv:0807.3959 [hep-ph]]; S. K. Majee, M. K. Parida, A. Raychaudhuri and U. Sarkar, Phys. Rev. D **75**, 075003 (2007) [arXiv:hep-ph/0701109]; N. Sahu and U. A. Yajnik, Phys. Rev. D **71**, 023507 (2005) [arXiv:hep-ph/0410075]; S. Khalil, arXiv:1004.0013 [hep-ph]; J. Chakraborty, arXiv:1003.3154 [hep-ph]; C. Wei, arXiv:1003.1468 [hep-ph]; P. S. B. Dev and R. N. Mohapatra, Phys. Rev. D **81**, 013001 (2010) [arXiv:0910.3924 [hep-ph]]; Z. z. Xing and S. Zhou, Phys. Lett. B **679**, 249 (2009) [arXiv:0906.1757 [hep-ph]]; M. Aoki, S. Kanemura and O. Seto, Phys. Rev. D **80**, 033007 (2009) [arXiv:0904.3829 [hep-ph]]; P. Ren and Z. z. Xing, Phys. Lett. B **666**, 48 (2008) [arXiv:0805.4292 [hep-ph]]; G. C. Cho, S. Kaneko and A. Omote, Phys. Lett. B **652**, 325 (2007) [arXiv:hep-ph/0611240]; E. J. Chun and S. Scopel, Phys. Rev. D **75**, 023508 (2007) [arXiv:hep-ph/0609259]; S. F. King and T. Yanagida, Prog. Theor. Phys. **114**, 1035 (2006) [arXiv:hep-ph/0411030]; A. Sarkar and U. A. Yajnik, Phys. Rev. D **76**, 025001 (2007) [arXiv:hep-ph/0703142]; K. Huitu, S. Khalil, H. Okada and S. K. Rai, Phys. Rev. Lett. **101**, 181802 (2008) [arXiv:0803.2799 [hep-ph]].
- [15] M. S. Carena, A. Daleo, B. A. Dobrescu and T. M. P. Tait, Phys. Rev. D **70**, 093009 (2004) [arXiv:hep-ph/0408098].
- [16] P. Langacker, arXiv:0911.4294 [hep-ph]; V. Barger, P. Langacker and H. S. Lee, Phys. Rev.

- Lett. **103**, 251802 (2009) [arXiv:0909.2641 [hep-ph]]; W. Emam and S. Khalil, Eur. Phys. J. C **522**, 625 (2007) [arXiv:0704.1395 [hep-ph]]; M. C. Chen and J. Huang, Phys. Rev. D **81**, 055007 (2010) [arXiv:0910.5029 [hep-ph]]; E. J. Chun, Phys. Rev. D **72** 095010 (2005) [arXiv:hep-ph/0508050].
- [17] T. Aaltonen *et al.* [CDF Collaboration], Phys. Rev. Lett. **102**, 091805 (2009) [arXiv:0811.0053 [hep-ex]].
- [18] See for a review: T. Schwetz, M. A. Tortola and J. W. F. Valle, New J. Phys. **10**, 113011 (2008) [arXiv:0808.2016 [hep-ph]].
- [19] D. Larson *et al.*, arXiv:1001.4635 [astro-ph.CO].
- [20] C. Amsler *et al.* (Particle Data Group), Phys. Lett. **B667**, 1 (2008).
- [21] J. Adam *et al.* [MEG collaboration], arXiv:0908.2594 [hep-ex].
- [22] L. Lavours, Eur. Phys. J.C. **29**, 191 (2003).
- [23] A.G. Akeroyd, M. Aoki, H. Sugiyama, Phys. Rev. D **79**, 113010 (2009).
- [24] A. G. Akeroyd and M. Aoki, Phys. Rev. D **72**, 035011 (2005) [arXiv:hep-ph/0506176].
- [25] K. Huitu, J. Maalampi, A. Pietila and M. Raidal, Nucl. Phys. B **487** (1997) 27 [arXiv:hep-ph/9606311].
- [26] E. Ma, M. Raidal and U. Sarkar, Nucl. Phys. B **615** (2001) 313 [arXiv:hep-ph/0012101].
- [27] A. Hektor, M. Kadastik, M. Muntel, M. Raidal and L. Rebane, Nucl. Phys. B **787** (2007) 198 [arXiv:0705.1495 [hep-ph]].
- [28] T. Rommerskirchen and T. Hebbeker, J. Phys. G **33** (2007) N47.
- [29] G. Azuelos, K. Benslama and J. Ferland, J. Phys. G **32** (2006) 73 [arXiv:hep-ph/0503096].
- [30] F. del Aguila and J. A. Aguilar-Saavedra, Nucl. Phys. B **813**, 22 (2009) [arXiv:0808.2468 [hep-ph]].
- [31] B. Dion, T. Gregoire, D. London, L. Marleau and H. Nadeau, Phys. Rev. D **59**, 075006 (1999) [arXiv:hep-ph/9810534].
- [32] M. Muhlleitner and M. Spira, Phys. Rev. D **68**, 117701 (2003) [arXiv:hep-ph/0305288].
- [33] T. Han, B. Mukhopadhyaya, Z. Si and K. Wang, Phys. Rev. D **76**, 075013 (2007) [arXiv:0706.0441 [hep-ph]].
- [34] J. Pumplin, D. R. Stump, J. Huston, H. L. Lai, P. M. Nadolsky and W. K. Tung, JHEP **0207** 012 (2002) [arXiv:hep-ph/0201195].
- [35] F. Maltoni and T. Stelzer, JHEP **0302**, 027 (2003) [arXiv:hep-ph/0208156].